Downloaded from geology.gsapubs.org on November 19, 2015

Extreme eolian delivery of reactive iron to late Paleozoic icehouse seas

Sohini Sur[1], Jeremy D. Owens[2,3], Gerilyn S. Soreghan[1]*, Timothy W. Lyons[2], Robert Raiswell[4], Nicholas G. Heavens[5], and Natalie M. Mahowald[6]

[1]School of Geology and Geophysics, University of Oklahoma, Norman, Oklahoma 73019, USA
[2]Department of Earth Sciences, University of California–Riverside, Riverside, California 92521, USA
[3]Earth, Ocean, and Atmospheric Science, Florida State University, Tallahassee, Florida 32306, USA
[4]School of Earth and Environment, University of Leeds, Leeds LS2 9JT, UK
[5]Department of Atmospheric and Planetary Sciences, Hampton University, Hampton, Virginia 23669, USA
[6]Department of Earth and Atmospheric Sciences, Cornell University, Ithaca, New York 14853, USA

ABSTRACT

The biogeochemical impacts of iron-rich dust to the oceans are known for Earth's recent record but unexplored for deep time, despite recognition of large ancient dust fluxes, particularly during the late Paleozoic. We report a unique Fe relationship for Upper Pennsylvanian mudrock of eolian origin that records lowstand (glacial) conditions within a carbonate buildup of western equatorial Pangaea (western United States) well removed from other detrital inputs. Here, reactive Fe unambiguously linked to dust is enriched without a corresponding increase in total Fe. More broadly, data from thick coeval loess deposits of western equatorial Pangaea show the same marked enrichment in reactive Fe. This enrichment—atypical compared to modern marine, fluvial, glacial, loess, and soil sediments—suggests an enhancement of the reactivity of the internal Fe pool that increased the bioavailability of the Fe for marine primary production. Regardless of the mechanism behind this enhancement, our data in combination with other evidence for high dust fluxes imply delivery of extraordinarily large amounts of biogeochemically reactive Fe to glacial-stage late Paleozoic seas, and modeling of this indicates major impacts on carbon cycling and attendant climatic feedbacks.

INTRODUCTION

In much of the modern ocean, iron is a limiting nutrient for marine primary productivity, which in turn influences atmospheric CO_2 (e.g., Martin et al., 1994; Boyd et al., 2007). Atmospheric dust is a key source of bioavailable Fe to the ocean (e.g., Jickells et al., 2005), despite uncertainty regarding the processes that enhance Fe bioavailability from dust (e.g., Mahowald et al., 2009; Raiswell and Canfield, 2012). Clarification of the role of Fe in ocean biogeochemistry thus remains a goal for the modern and recent, and is completely unexplored for Earth's deep-time record.

The role of Fe in ancient ecosystems is elucidated by techniques enabling identification of three Fe pools within the total Fe (Fe_T) pool: highly reactive (Fe_{HR}), poorly reactive, and unreactive (Canfield, 1989; Raiswell et al., 1994; Raiswell and Canfield, 1998; Poulton and Canfield, 2005). Fe_{HR} in mineral dust consists predominantly of amorphous and crystalline iron oxides and (oxyhydr)oxides. These phases are most likely to have been soluble and thus bioavailable at the time of deposition. This original Fe_{HR} is present in ancient dust dominantly as crystalline oxides, soluble in a citrate-bicarbonate–buffered sodium dithionite (CBD) solution (Fe_D). In some cases, a portion of those oxides may have been diagenetically transformed to pyrite (Fe_{py}). If the crystalline oxide phases extracted from the geologic record at least partially reflect less-crystalline, more-soluble oxyhydroxide bioavailable precursors such as ferrihydrite, then ancient Fe_{HR} correspondingly scales to initial bioavailability and thus can be used as a proxy for primary productivity, assuming ancient oceans had Fe-limited regions like today's oceans.

This scaling assumes that initial bioavailable Fe would have converted diagenetically to crystalline oxides and can never be measured directly in ancient sediment. Furthermore, prior to deposition, these phases would have been amenable to enhanced secondary bioavailability though photochemical or cloud/aerosol processing during eolian transport (Shi et al., 2012). An accurate measure of initial bioavailability for Fe phases buried, recrystallized, and now preserved remains a challenge even for the modern, but our approach advances this goal. Here, we assess Fe reactivity from Pennsylvanian glacial-stage dust preserved in an isolated reef and in paleo-loesses of greater western equatorial Pangaea (western United States). Collectively, these findings suggest remarkable fluxes of highly reactive Fe that should have profoundly influenced biogeochemical cycling of the late Paleozoic.

GEOLOGICAL BACKGROUND AND METHODS

During Pennsylvanian–Permian time, highlands and basins of the Ancestral Rocky Mountains formed in western tropical Pangaea (Figs. 1A and 1B). Strata within this greater region include the thickest (>700 m) dust/loess deposits

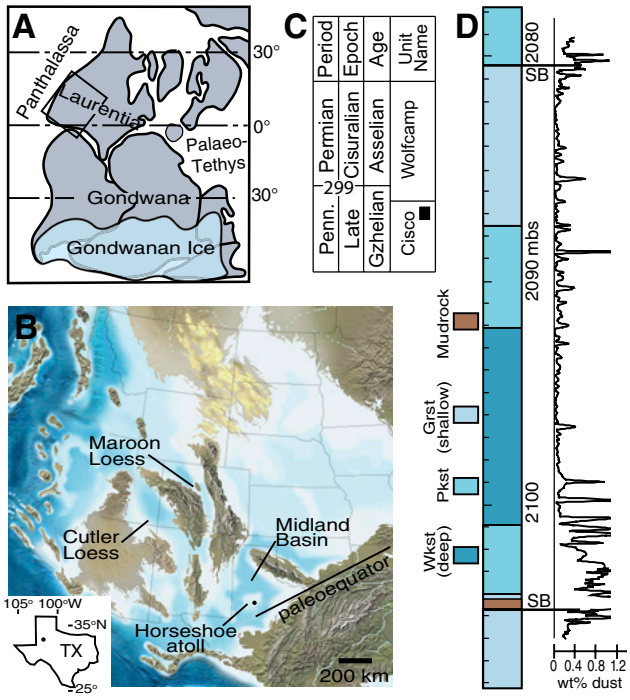

Figure 1. A: Late Paleozoic Pangaea, showing (boxed) region of interest in western tropical Pangaea (western USA; detailed in B). B: Part of paleogeographic map of North America for 300 Ma (from Blakey, 2013). Map depicts highstand conditions, with many epeiric seas (light blue colors); epeiric regions, including Horseshoe atoll, were exposed during lowstand (glacial) conditions. Core location is depicted with black circle. TX—Texas. C: Chronostratigraphy of Horseshoe atoll study interval (Cisco unit; designated by black box). Penn.—Pennsylvanian. D: Facies log and dust content (in wt%) of Horseshoe atoll study sequence (see Sur et al., 2010a). Blue colors are carbonate facies (deeper hues depict deeper-water facies). "SB" (sequence boundary) denotes lowstand (glacial) exposure surfaces. mbs—meters below surface; Wkst—wackestone; Pkst—packstone; Grst—grainstone.

*E-mail: lsoreg@ou.edu

© 2015 Geological Society of America. For permission to copy, contact editing@geosociety.org.

Downloaded from geology.gsapubs.org on November 19, 2015

yet documented on Earth (Soreghan et al., 2008), and marine carbonate in epeiric systems. One such epeiric system, the Midland Basin, contains Horseshoe atoll, an isolated Upper Pennsylvanian–Lower Permian algal reef (Fig. 1B) devoid of siliciclastic material excepting that delivered via eolian input (Sur et al., 2010a). The provenance of this dust indicates continental sources (e.g., Ancestral Rocky Mountains uplifts) with minor contributions from the Ouachita orogen (Sur et al., 2010a). An important implication of this setting is that chemical fingerprints of this dust and its inferred bioavailability can be extrapolated to the vast loess and dust deposits preserved in the coeval continental record. Furthermore, these large volumes of continental dust suggest that parts of the ocean received similarly large Fe inputs (Large et al., 2015; Soreghan et al., 2015) with analogous bioreactivity. The section (Cisco unit) at Horseshoe atoll contains several glacioeustatic sequences (~18–24 m thick) separated by paleosols recording glacial (lowstand) conditions that exposed the buildups to dust fall, much like the Bahamian reef incorporates Saharan dust today. The middle Gzhelian (Upper Pennsylvanian) interval consists predominantly (99%) of carbonate, with <1% siliciclastic mudrock concentrated at sequence boundaries (Sur et al., 2010a). We highlight analyses on the sequence-bounding, glacial-stage mudrock from two sequences. The section is subsurface, hence we used a continuous, air-drilled core. For dust extraction, 50 g samples were crushed to pea size and treated with HCl for carbonate removal, combustion for organic removal, and CBD for Fe-oxide removal (Sur et al., 2010b). To assess Fe_T, samples were powdered and dissolved using a standard multi-acid digestion for total elemental concentrations using an inductively coupled plasma–mass spectrometer (ICP-MS). A split was used to analyze Fe-pyrite contents and pyrite S isotopes using a standard chromium reduction method. A sequential Fe extraction was done to measure Fe-carbonates, Fe-oxides, and Fe-magnetite (see the GSA Data Repository[1] for additional details).

SEDIMENTOLOGIC OVERVIEW AND GEOCHEMICAL DATA

Figure 1D details the weight percent of siliciclastic dust extracted through one sequence and highlights the mudrock that occurs atop a (glacial-stage) exposure surface (sequence boundary). This boundary is marked by pedogenic calcrete and root traces (Sur et al., 2010a; Fig. 2A) in sharp contact with subtidal carbonate above and below. Within the mudrock, subangular blocky microstructures, pedotubules, clay coatings, and localized centimeter-scale slickensides mark pedogenesis (Fig. 2B); additionally, euhedral pyrite crystals and aggregates (spore pseudomorphs) are common (Fig. 2C). Quartz and illite are the dominant components. Modal grain size is 5 µm (mean = 6 µm; median = 5.5 µm).

Five samples through the ~0.4 m mudrock were analyzed for bulk-rock geochemistry (ICP-MS), total organic carbon (TOC), total sulfur (S_T), dithionite-soluble Fe concentration (Fe_D), pyrite S concentration (S_{py}), and pyrite S isotope composition ($\delta^{34}S_{py}$). Fe_{HR} is determined by summing Fe_D and Fe_{py} (Poulton and Canfield, 2005), yielding ratios of Fe_{HR} to Fe_T ranging from 0.66 to 0.78 (Table 1; Fig. 3). Very low inorganic carbon contents of <0.1 wt% confirm that Fe associated with carbonate is negligible. Magnetite Fe was not analyzed; however, the addition of magnetite would only increase Fe_{HR}/Fe_T but not affect total Fe values. The Fe_{HR}/Fe_T values are appreciably higher than those reported from modern riverine particulates (average 0.43 ± 0.03; Poulton and Raiswell, 2002), oxic and dysoxic continental margin and deep-sea sediments (0.26 ± 0.09; Anderson and Raiswell, 2004), and Saharan soil dust (0.33 ± 0.01; Poulton and Raiswell, 2002; cf. Shi et al., 2012). Rather, they are more typical of ratios in modern euxinic (anoxic and sulfidic) settings, such as the Black Sea and the Cariaco Basin (offshore Venezuela) (Raiswell and Canfield, 1998). By contrast, the Fe_T/Al of the studied section ranges from 0.32 to 0.41 (average 0.36; Fig. 3), which is low compared to average Fe_T/Al (0.53) of Paleozoic shale (Raiswell et al., 2011) and average continental crust (upper continental crust [UCC]; Taylor and McLennan, 1985), and significantly lower than modern euxinic sediments in the Black Sea (mean 0.89 ± 0.16; Lyons and Severmann, 2006). The mudrock contains very low TOC (0.13–0.25 wt%) yet high pyrite S (2.01–3.01 wt%). $\delta^{34}S_{py}$ ranges from +1.20‰ to +10.80‰, relative to +12‰ for coeval seawater sulfate (Table 1; Kampschulte and Strauss, 2004). In comparison, Fe_{HR}/Fe_T of coeval (Upper Pennsylvanian–Lower Permian) loess and intercalated pedogenically modified loess in western tropical Pangaea (e.g., paleoloess of the Maroon and Cutler Formations) also show elevated Fe_{HR}/Fe_T values (Fig. 3) with Fe_T/Al values that overlap with the data from Horseshoe atoll.

Importantly, sedimentologic and paleogeographic attributes indicate that the mudrock from the atoll originated as dust. It consists of non-biogenic, fine silt and clay composed of detrital quartz and clay minerals, which accumulated atop an isolated carbonate pinnacle that stood as much as 600 m (Burnside, 1959) above the surrounding seafloor during growth. The paleogeographic isolation precludes an origin for the mudrock from fluviodeltaic or deepwater clastics, and the mineralogy precludes a volcanic source. The mudrock exhibits weak pedogenesis (e.g., slickensides) and lacks horizonation, recording immature pedogenesis.

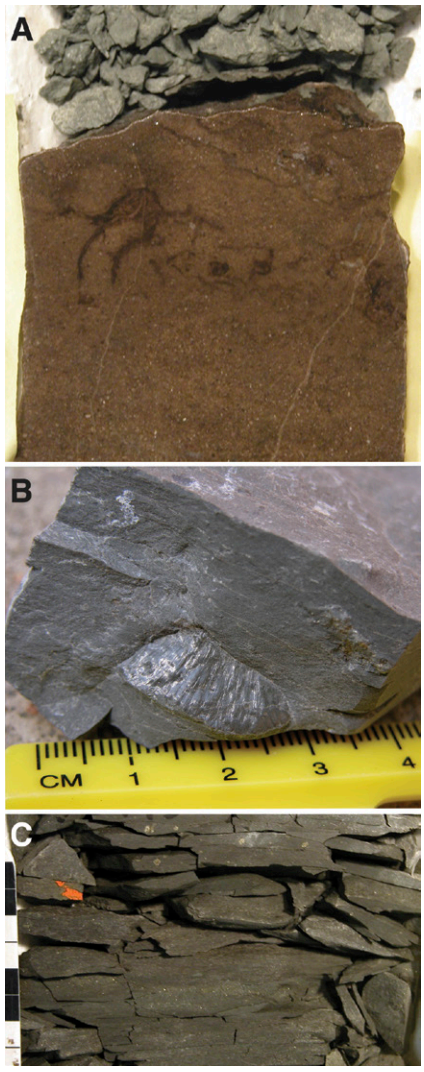

Figure 2. Sedimentary attributes of sequence-boundary mudrock. A: Sequence boundary at ~2104 m (Fig. 1C). Note rhizoliths at left center (within subtidal carbonate). Core is ~8 cm wide. B: Slickenside surface within sequence-boundary mudrock. C: Pyrite (disseminated) in sequence-boundary mudrock (centimeter scale at left shows 4 cm).

Differential compaction around pyrite grains confirms their early diagenetic origin, most readily linked to sulfate supplied by seawater seepage during transgression subsequent to dust accumulation (cf. Wright, 1986)—a model supported by the marine-like $\delta^{34}S_{py}$ values. Analogous ^{34}S enrichments are associated with secondary sulfate diffusion and concomitant Rayleigh distillation effects from bacterial sulfate reduction during recent glacial-interglacial

[1]GSA Data Repository item 2015366, details on dust sampling and locations for all samples, Fe and Al data for samples in Figure 3, and additional methods details for laboratory and modeling aspects, is available online at www.geosociety.org/pubs/ft2015.htm, or on request from editing@geosociety.org or Documents Secretary, GSA, P.O. Box 9140, Boulder, CO 80301, USA.

Downloaded from geology.gsapubs.org on November 19, 2015

TABLE 1: GEOCHEMICAL DATA FOR HORSESHOE ATOLL MUDROCK (DUST) SAMPLES

Sample number	Depth (m)	TOC (%)	S_{py} (%)	Fe_T (%)	Fe_{py} (%)	Fe_D (%)	Fe_{HR} (%)	Fe_{HR}/Fe_T	Fe_T/Al	$\delta^{34}S_{py}$ (‰)
S-2	2104.36	0.21	1.91	2.55	1.67	0.12	1.78	0.70	0.33	9.6
S-4	2104.41	0.15	1.93	2.56	1.68	0.13	1.81	0.71	0.32	10.8
S-8	2104.50	0.25	2.82	3.31	2.46	0.13	2.58	0.78	0.41	1.2
S-12	2104.60	0.18	2.02	2.88	1.77	0.14	1.90	0.66	0.36	6.7
S-16	2104.69	0.13	2.50	3.2	2.17	0.01	2.19	0.68	0.40	5.3

Note: TOC—total organic carbon; S_{py}—pyrite sulfur; Fe_T—total iron; Fe_{py}—pyrite iron; Fe_D—dithionite iron; Fe_{HR}—highly reactive iron.

transitions from freshwater lacustrine to marine conditions (Jørgensen et al., 2004). These $\delta^{34}S_{py}$ values contrast with the strongly negative values typifying pyrite formation in marine sediments and water columns (e.g., Lyons, 1997). As the mudrock contains very low TOC, a reasonable electron donor for the sulfate reduction could be methane, diffusing from known organic-rich basinal facies. Regardless, the key consideration is that the pyrite formed dominantly from Fe-oxides originally deposited with the dust, and thus pyrite Fe should be included in our calculation of dust-derived Fe_{HR}. In other words, Fe_{HR} acts as a proxy for original oxide content. Importantly, glacial-stage dust flux to the study region exceeded that of interglacials by a factor of 400–4000, using estimated mass accumulation rates (see Sur et al., 2010a).

IRON FLUXES AND CYCLING IN THE LATE PALEOZOIC OCEAN

In light of the eolian origin, we can explore the Fe relationships for the mudrock with an eye toward the possibility of enhanced delivery of reactive Fe and its potential biological impact. The high values of Fe_{HR}/Fe_T in Horseshoe atoll are 2–3 times averages reported from river and oxic marine sediments (Raiswell and Canfield, 1998; Poulton and Raiswell, 2002) and considerably enriched compared to modern Saharan dust (Fig. 3). Processes operating during typical transport (fluvial *and* eolian) and marine processes thus fail to explain the unusual combination of elevated Fe_{HR} without overall Fe enrichments relative to average continental sources.

One model for Fe_{HR} enrichment, without concomitant increases in Fe_T/Al, is post-depositional weathering (pedogenesis). However, the weak evidence for pedogenesis indicates minimal in situ weathering. Additionally, Upper Pennsylvanian–Lower Permian dust samples generally exhibit higher Fe_{HR}/Fe_T (0.53, $n = 71$) compared to pedogenically altered equivalents (0.41, $n = 24$) within the same strata (Fig. 3), suggesting that Fe_{HR} was instead leached during pedogenesis. Our discovery of a fingerprint of elevated Fe_{HR}/Fe_T in the absence of overall Fe enrichment suggests repartitioning of unreactive to reactive Fe via as-yet poorly understood processing that also enhanced its bioreactivity. Recall that our estimate of reactivity is limited, because of the age of the sediments, to initial Fe-oxide content of the dust. However, relatively high Fe-oxide content in ancient dust is compatible with proportionally high bioavailability via enhancement that likely operated during transport.

Various processes have been suggested to effect enrichment of Fe_{HR} and presumably bioreactivity of iron in atmospheric dust. Some evidence points to size fractionation, with finer sizes variably enriched (e.g., Poulton and Raiswell, 2005; Poulton and Canfield 2005; Shi et al., 2011), although Buck et al. (2010) found no increase in Fe solubility with decreasing particle size in Atlantic aerosols. Regardless, size fractionation fails to explain our data, as both the Paleozoic loess and marine mudrock exhibit high Fe_{HR}, yet they span modes ranging from coarse silt to fine silt/clay. Others have suggested mineralogical controls, wherein clay-derived Fe is more soluble than Fe from other minerals (Journet et al., 2008; Shi et al., 2011). However, although our marine mudrock is clay rich relative to the other Paleozoic loess, all show high reactivity. Thus, we favor atmospheric processing known to be important in enhancing bioreactivity through, for example, photoreduction of Fe(III) to Fe(II) (Kim et al., 2010), evaporation and attendant acidification during cloud/aerosol processing (Jickells and Spokes, 2001), and other atmospheric processing (Shi et al., 2012). However, final answers are beyond the scope of this study, but the data imply a level of atmospheric processing in the late Paleozoic that exceeded modern levels.

The biological importance of Fe lies with its solubility and thus its bioavailability. Regardless of the mechanism for enrichment of Fe_{HR} in this late Paleozoic data set, the data demonstrate high values of highly reactive Fe, and previous analyses indicate extreme glacial-stage dust fluxes (Sur et al., 2010a). The large fluxes suggest remarkable atmospheric dust loading, an inference corroborated by the vast paleo-loess deposits of the Pennsylvanian–Permian—the thickest documented in the geologic record (Soreghan et al., 2008). While paleo-loess deposits so far only have been identified near the equator, using coal mineral matter as a dust proxy suggests significant dust deposition in Angara, North China, and West Gondwana even during interglacial intervals of the Permian, implying a global impact for dust (Large et al., 2015). Importantly, we can imagine vast coeval delivery of similarly bioavailable Fe to the oceans.

Integrating these results with aerosol modeling simulations for Early Permian paleogeography (Soreghan et al., 2015) yields estimates of 14–120 Pg/yr of carbon fixation attributable to dust fertilization—or 2–16 times the estimated modern marine carbon fixation attributable to dust fertilization (Okin et al., 2011; see the Data Repository for mass balance details). The car-

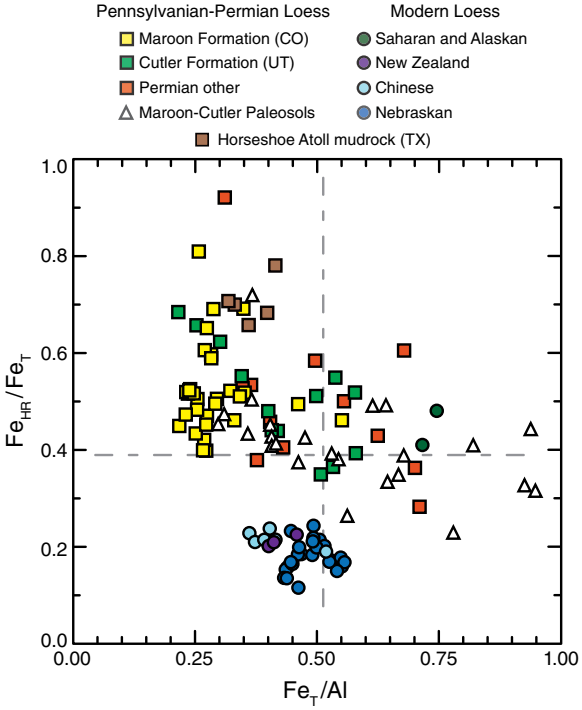

Figure 3. Cross plot of Fe_{HR}/Fe_T (highly reactive Fe/total Fe) versus Fe_T/Al illustrates enrichment of reactive Fe from Horseshoe atoll mudrock (brown squares) in relation to approximately coeval loess of (primarily) western tropical Pangaea (Maroon and Cutler Formations of Colorado [CO] and Utah [UT], USA) and their pedogenically altered equivalents (triangles). Orange squares are Permian paleo-loess from several other regions, including western USA (Oklahoma and New Mexico). Circles represent values from modern dust and loess samples as indicated (our unpublished data). Horizontal and vertical dashed lines are average continental values for Fe_{HR}/Fe_T and Fe_T/Al, respectively. TX—Texas. All data, with exception of Horseshoe atoll mudrock, include dithionite Fe, magnetite Fe, and pyrite Fe, which collectively compose the Fe_{HR} pool.

Downloaded from geology.gsapubs.org on November 19, 2015

bon isotope expression of the high levels of organic production expected with enhanced Fe_{HR} delivery to the ocean and associated impact on CO_2 levels in the atmosphere could be masked by the large amounts of terrestrial organic burial during this interval. However, our results have important implications for both deep-time and modern climate change and thus merit further exploration and testing.

ACKNOWLEDGMENTS

Sur was funded in part by the Petroleum Research Fund (PRF #39198-AC8) and the National Science Foundation, including the following: to Soreghan—EAR-0746042, EAR-1053018, and EAR-1338331 (latter from the ELT program); to Lyons (funding Owens)—EAR-0745602; to Mahowald (funding Heavens)—EAR-0745961, EAR-0932946, and EAR-1003509; and to Heavens EAR-1337363 (from the ELT program). We thank A. Saller, G. Hinterlong, A. Auffant, and S. Randall for core access; M. Soreghan and A. Saller for discussions; and C. Scott, S. Bates, and A. Gerhardt (UCR) for laboratory assistance. Finally, we thank *Geology* Editor E. Thomas, reviewers K. Tierney and A. Derkowski, and three anonymous reviewers for constructive comments on earlier versions of this manuscript. We dedicate this work to the memory of Rich Lane, a tireless advocate for the science of the Earth system as contained within the sedimentary crust.

REFERENCES CITED

Anderson, T.F., and Raiswell, R., 2004, Sources and mechanisms for the enrichment of highly reactive iron in euxinic Black Sea sediments: American Journal of Science, v. 304, p. 203–233, doi:10.2475/ajs.304.3.203.

Blakey, R., 2013, North American paleogeographic map, 300 Ma: Phoenix, Arizona, Colorado Plateau Geosystems, http://cpgeosystems.com/paleomaps.html (accessed October 2014).

Boyd, P.W., et al., 2007, Mesoscale iron enrichment experiments 1993–2005: Synthesis and future directions: Science, v. 315, p. 612–617, doi:10.1126/science.1131669.

Buck, C.S., Landing, W.M., and Resing, J.A., 2010, Particle size and aerosol iron solubility: A high-resolution analysis of Atlantic aerosols: Marine Chemistry, v. 120, p. 14–24, doi:10.1016/j.marchem.2008.11.002.

Burnside, R.J., 1959, Geology of part of the Horseshoe Atoll in Borden and Howard Counties, Texas: U.S. Geological Survey Professional Paper 315-B, 34 p.

Canfield, D.E., 1989, Reactive iron in marine sediments: Geochimica et Cosmochimica Acta, v. 53, p. 619–632, doi:10.1016/0016-7037(89)90005-7.

Jickells, T., and Spokes, L., 2001, Atmospheric iron inputs to the oceans, *in* Turner, D.R., and Hunteger, K., eds., Biogeochemistry of Iron in Seawater: Chichester, UK, John Wiley and Sons, Ltd., p. 85–121.

Jickells, T.D., et al., 2005, Global iron connections between desert dust, ocean biogeochemistry, and climate: Science, v. 308, p. 67–71, doi:10.1126/science.1105959.

Jørgensen, B.B., Bottcher, M.E., Luschen, H., Neretin, L.N., and Volkov, I.I., 2004, Anaerobic methane oxidation and a deep H_2S sink generate isotopically heavy sulfides in Black Sea sediments: Geochimica et Cosmochimica Acta, v. 68, p. 2095–2118, doi:10.1016/j.gca.2003.07.017.

Journet, E., Desboeufs, K.V., Caquineau, S., and Colin, J.-L., 2008, Mineralogy as a critical factor of dust iron solubility: Geophysical Research Letters, v. 35, L07805, doi:10.1029/2007GL031589.

Kampschulte, A., and Strauss, H., 2004, The sulfur isotopic evolution of Phanerozoic sea water based on the analysis of structurally substituted sulfate in carbonates: Chemical Geology, v. 204, p. 255–286, doi:10.1016/j.chemgeo.2003.11.013.

Kim, K., Choi, W., Hoffman, M.R., Yoon, H.-I., and Park, B.-K., 2010, Photoreductive dissolution of iron oxides trapped in ice and its environmental implications: Environmental Science & Technology, v. 44, p. 4142–4148, doi:10.1021/es9037808.

Large, D.J., Marshall, C., and Heavens, N., 2015, Coal-derived rates of atmospheric dust deposition over Pangea during the Permian: Gondwana Research, doi:10.1016/j.gr.2015.10.002 (in press).

Lyons, T.W., 1997, Sulfur isotopic trends and pathways of iron sulfide formation in upper Holocene sediments of the anoxic Black Sea: Geochimica et Cosmochimica Acta, v. 61, p. 3367–3382, doi:10.1016/S0016-7037(97)00174-9.

Lyons, T.W., and Severmann, S., 2006, A critical look at iron paleoredox proxies: New insights from modern euxinic marine basins: Geochimica et Cosmochimica Acta, v. 70, p. 5698–5722, doi:10.1016/j.gca.2006.08.021.

Mahowald, N.M., et al., 2009, Atmospheric iron deposition, global distribution, variability, and human perturbations: Annual Review of Marine Science, v. 1, p. 245–278, doi:10.1146/annurev.marine.010908.163727.

Martin, J.H., et al., 1994, Testing the iron hypothesis in ecosystems of the equatorial Pacific Ocean: Nature, v. 371, p. 123–129, doi:10.1038/371123a0.

Okin, G.S., et al., 2011, Impacts of atmospheric nutrient deposition on marine productivity: Roles of nitrogen, phosphorus, and iron: Global Biogeochemical Cycles, v. 25, GB2022, doi:10.1029/2010GB003858.

Poulton, S.W., and Canfield, D.E., 2005, Development of a sequential extraction procedure for iron: Implications for iron partitioning in continentally derived particulates: Chemical Geology, v. 214, p. 209–221, doi:10.1016/j.chemgeo.2004.09.003.

Poulton, S.W., and Raiswell, R., 2002, The low-temperature geochemical cycle of iron: From continental fluxes to marine sediment deposition: American Journal of Science, v. 302, p. 774–805, doi:10.2475/ajs.302.9.774.

Poulton, S.W., and Raiswell, R., 2005, Chemical and physical characteristics of iron oxides in riverine and glacial meltwater sediments: Chemical Geology, v. 218, p. 203–221, doi:10.1016/j.chemgeo.2005.01.007.

Raiswell, R., and Canfield, D.E., 1998, Sources of iron for pyrite formation in marine sediments: American Journal of Science, v. 298, p. 219–245, doi:10.2475/ajs.298.3.219.

Raiswell, R., and Canfield, D.E., 2012, The iron biogeochemical cycle past and present: Geochemical Perspectives, v. 1, p. 1–220, doi:10.7185/geochempersp.1.1.

Raiswell, R., Canfield, D.E., and Berner, R.A., 1994, A comparison of iron extraction methods for the determination of degree of pyritisation and the recognition of iron-limited pyrite formation: Chemical Geology, v. 111, p. 101–110, doi:10.1016/0009-2541(94)90084-1.

Raiswell, R., Reinhard, C.T., Derkowski, A., Owens, J., Bottrell, S.H., Anbar, A.D., and Lyons, T.W., 2011, Formation of syngenetic and early diagenetic iron minerals in the late Archean Mt. McRae Shale, Hamersley Basin, Australia: New insights on the patterns, controls, and paleoenvironmental implications of authigenic mineral formation: Geochimica et Cosmochimica Acta, v. 75, p. 1072–1087, doi:10.1016/j.gca.2010.11.013.

Shi, Z., et al., 2011, Influence of chemical weathering and aging of iron oxides on the potential iron solubility of Saharan dust during simulated atmospheric processing: Global Biogeochemical Cycles, v. 25, GB2010, doi:10.1029/2010GB003837.

Shi, Z., Krom, M.D., Jickells, T.D., Bonneville, S., Carslaw, K.S., Mihalopoulos, N., Baker, A.R., and Benning, L.G., 2012, Impacts on iron solubility in the mineral dust by processes in the source region and the atmosphere: A review: Aeolian Research, v. 5, p. 21–42, doi:10.1016/j.aeolia.2012.03.001.

Soreghan, G.S., Soreghan, M.J., and Hamilton, M.A., 2008, Origin and significance of loess in late Paleozoic western Pangaea: A record of tropical cold?: Palaeogeography, Palaeoclimatology, Palaeoecology, v. 268, p. 234–259, doi:10.1016/j.palaeo.2008.03.050.

Soreghan, G.S., Heavens, N.G., Hinnov, L.A., Aciego, S.M., and Simpson, C., 2015, Reconstructing the dust cycle in deep time: The case of the late Paleozoic icehouse, *in* Polly, P.D., et al., eds., Earth-Life Transitions: Paleobiology in the Context of Earth System Evolution: The Paleontological Society Papers v. 21, p. 83–120.

Sur, S., Soreghan, G.S., Soreghan, M.J., Yang, W., and Saller, A.H., 2010a, A record of glacial aridity and Milankovitch-scale fluctuations in atmospheric dust from the Pennsylvanian tropics: Journal of Sedimentary Research, v. 80, p. 1046–1067, doi:10.2110/jsr.2010.091.

Sur, S., Soreghan, M.J., Soreghan, G.S., and Stagner, A.F., 2010b, Extracting the silicate mineral fraction from ancient carbonate: Assessing the geologic record of dust: Journal of Sedimentary Research, v. 80, p. 763–769, doi:10.2110/jsr.2010.068.

Taylor, S.R., and McLennan, S.M., 1985, The Continental Crust: Its Composition and Evolution: Oxford, UK, Blackwell, 312 p.

Wright, V.P., 1986, Pyrite formation and the drowning of a paleosol: Geological Journal, v. 21, p. 139–149, doi:10.1002/gj.3350210205.

Manuscript received 4 August 2015
Revised manuscript received 9 October 2015
Manuscript accepted 12 October 2015

Printed in USA

Downloaded from geology.gsapubs.org on November 19, 2015

Geology

Extreme eolian delivery of reactive iron to late Paleozoic icehouse seas

Sohini Sur, Jeremy D. Owens, Gerilyn S. Soreghan, Timothy W. Lyons, Robert Raiswell, Nicholas G. Heavens and Natalie M. Mahowald

Geology 2015;43;1099-1102
doi: 10.1130/G37226.1

Email alerting services click www.gsapubs.org/cgi/alerts to receive free e-mail alerts when new articles cite this article

Subscribe click www.gsapubs.org/subscriptions/ to subscribe to Geology

Permission request click http://www.geosociety.org/pubs/copyrt.htm#gsa to contact GSA

Copyright not claimed on content prepared wholly by U.S. government employees within scope of their employment. Individual scientists are hereby granted permission, without fees or further requests to GSA, to use a single figure, a single table, and/or a brief paragraph of text in subsequent works and to make unlimited copies of items in GSA's journals for noncommercial use in classrooms to further education and science. This file may not be posted to any Web site, but authors may post the abstracts only of their articles on their own or their organization's Web site providing the posting includes a reference to the article's full citation. GSA provides this and other forums for the presentation of diverse opinions and positions by scientists worldwide, regardless of their race, citizenship, gender, religion, or political viewpoint. Opinions presented in this publication do not reflect official positions of the Society.

Notes

© 2015 Geological Society of America

THE
GEOLOGICAL
SOCIETY
OF AMERICA